nature research

https://doi.org/10.1038/s41561-019-0330-x

Supplementary information

Shape of (101955) Bennu indicative of a rubble pile with internal stiffness

In the format provided by the authors and unedited

Shape of (101955) Bennu indicative of a rubble pile with internal stiffness:

Supplementary Figures

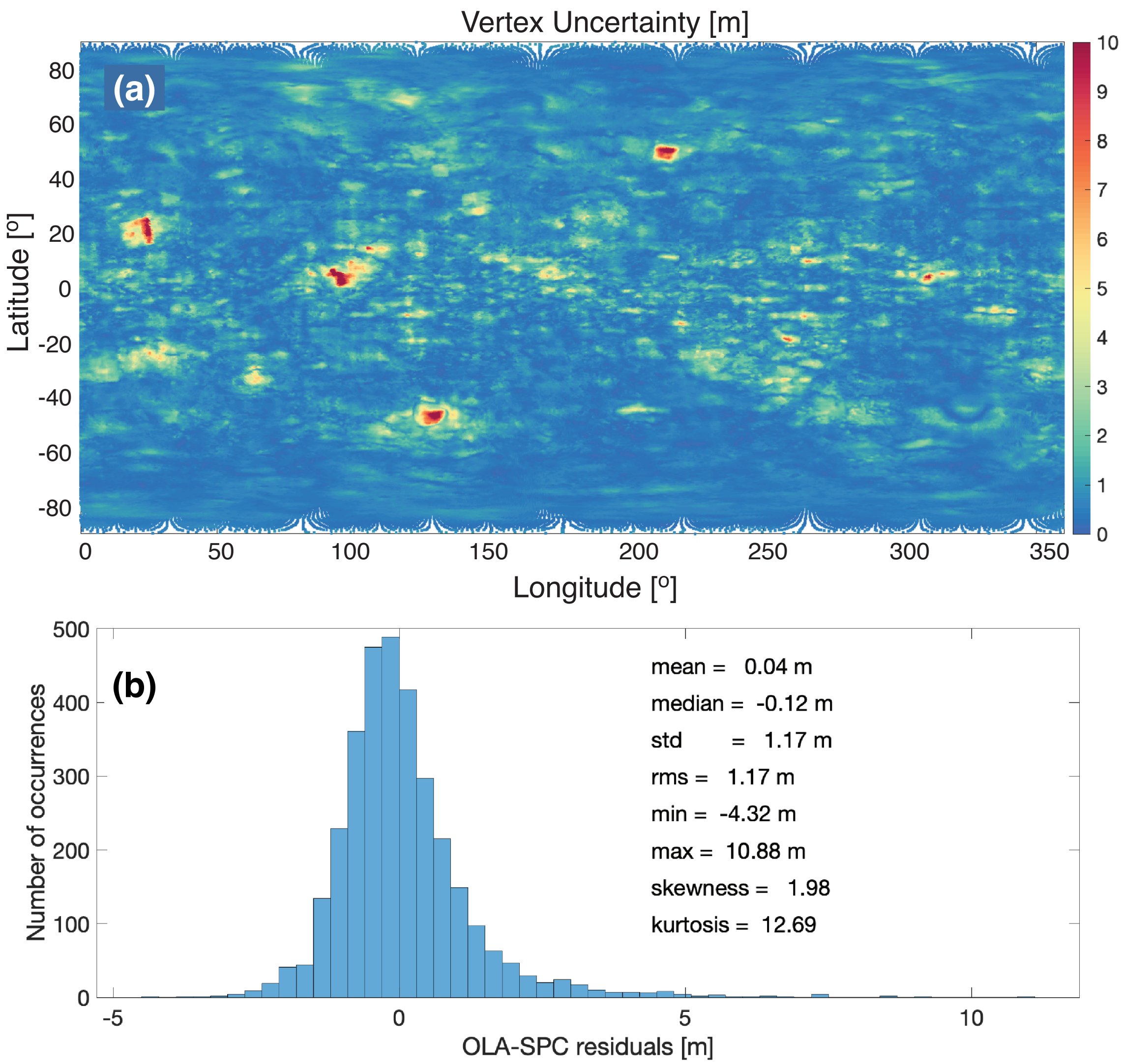

Supplementary Figure 1: Model Uncertainty: A map of radial uncertainty in the SPC-derived shape model is shown in **a**. The map is derived from the internal agreement of the SPC solutions scaled to an absolute accuracy using OLA data in **b**, which shows the residuals from comparing OLA returns with the SPC-derived model. This map represents a conservative estimate of the uncertainty and we expect any deviations from the model to fall within the values reported. The median difference in **b** is representative of the uncertainty in the overall extent of the GDTM, after the evaluation of a wide range of data, from limb information to stereo derived vectors, and tracking of surface landmarks during the early stages of the orbital phase around Bennu.

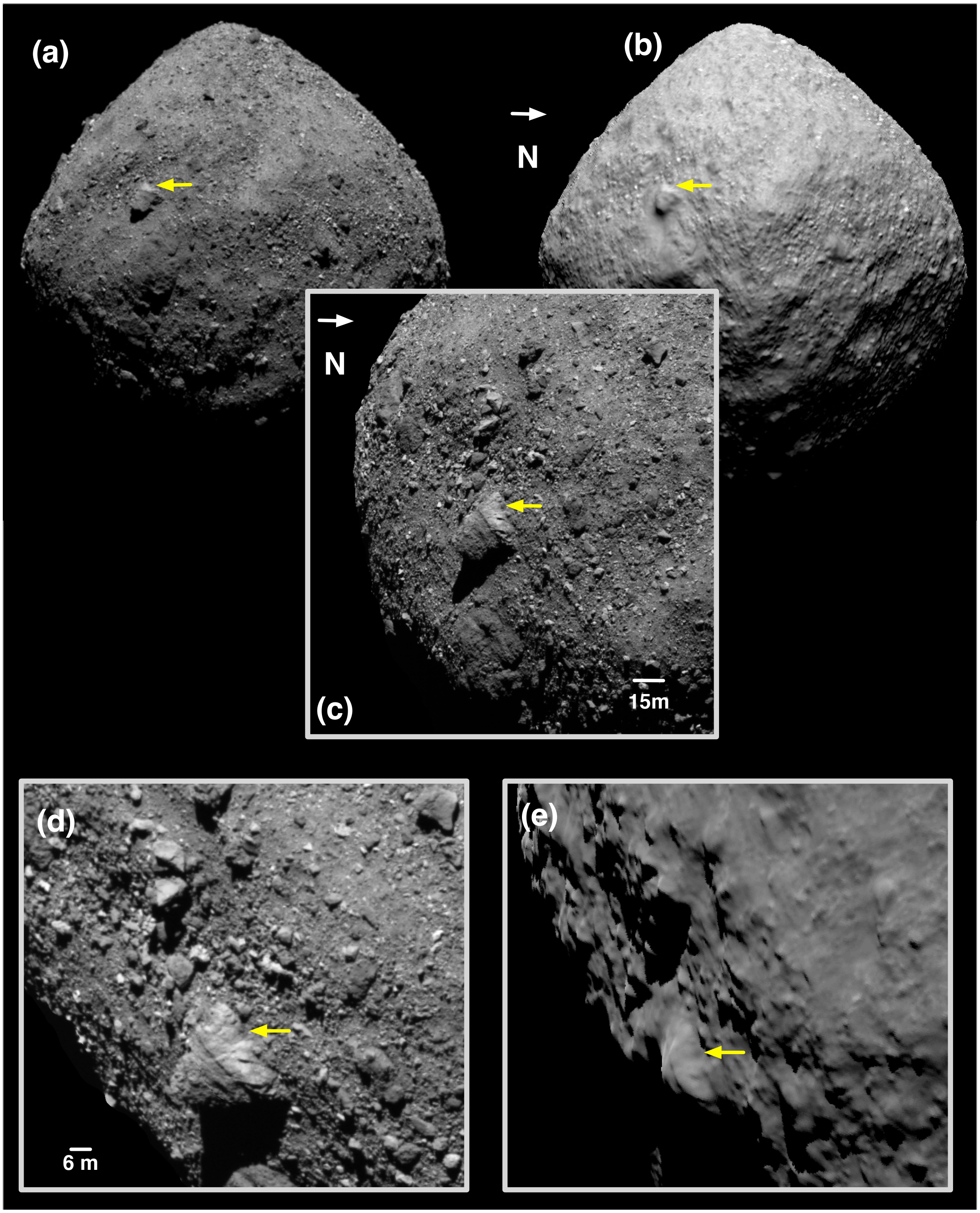

Supplementary Figure 2: The definition of the prime meridian for Bennu: The yellow arrows in the OCAMS images (a, collected on 13 December 2018 at 03:39:07 UTC; c, 02 December 2018 at 06:07:44 UTC) and the Bennu GDTM (b) indicate the location of the dark albedo patch on a large rock defining the prime meridian identified by the OSIRIS-REx science team. The dark patch is evident in higher resolution images (d, 01 December 2018 at 08:49:56 UTC) and in the rendering **e** of the shape model that include the relative albedo solution estimated by the SPC process. This point is located at 25.0ºS**.**

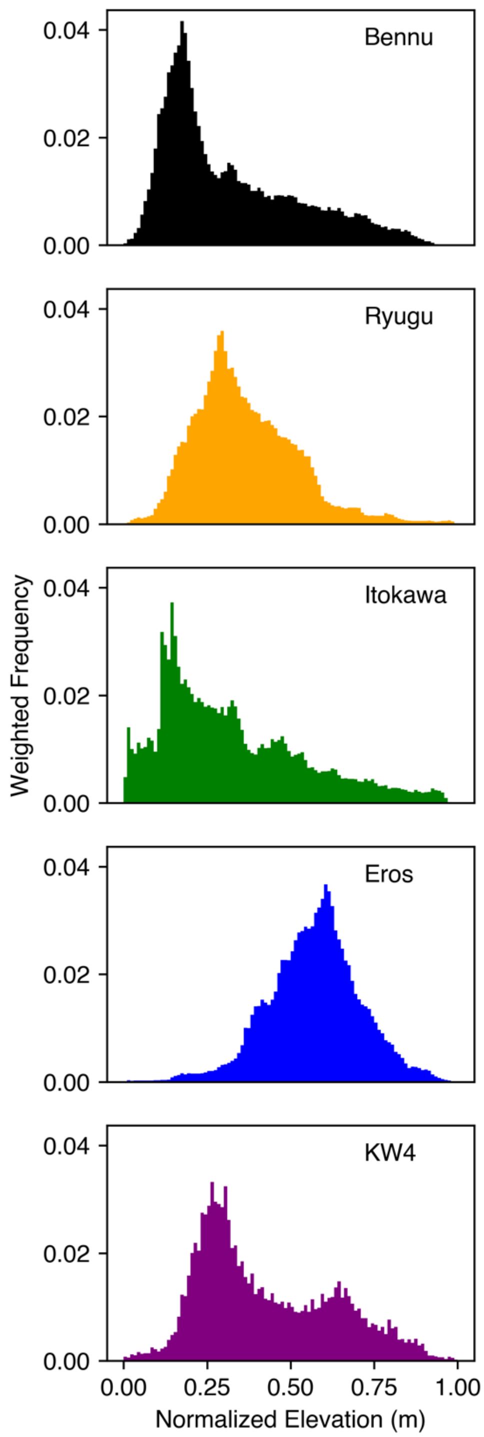

Supplementary Figure 3. Hypsometry plots showing normalized elevation for several near-Earth asteroids: To compute normalized elevation, the elevation of each facet in each asteroid's shape model was divided by the global range of elevation (i.e., maximum elevation - minimum elevation). Zero was set for each model to be equal to the minimum elevation divided by the elevation range. The contribution of each facet to the histogram was scaled by facet area normalized to the total surface area of the shape model. This transformation rescales the elevation of each body from 0 to 1 but preserves the overall shape of the elevation distribution for each body, thereby facilitating comparisons among the various asteroids. The hypsometry distribution of Bennu shows a secondary peak near a normalized elevation of ~0.3 that corresponds to the relatively high-standing longitudinal ridges. These are based on the following shape models: Eros [40], Itokawa [41], Ryugu [9], Bennu, and KW4A (https://echo.jpl.nasa.gov/asteroids/shapes/kw4a.obj).

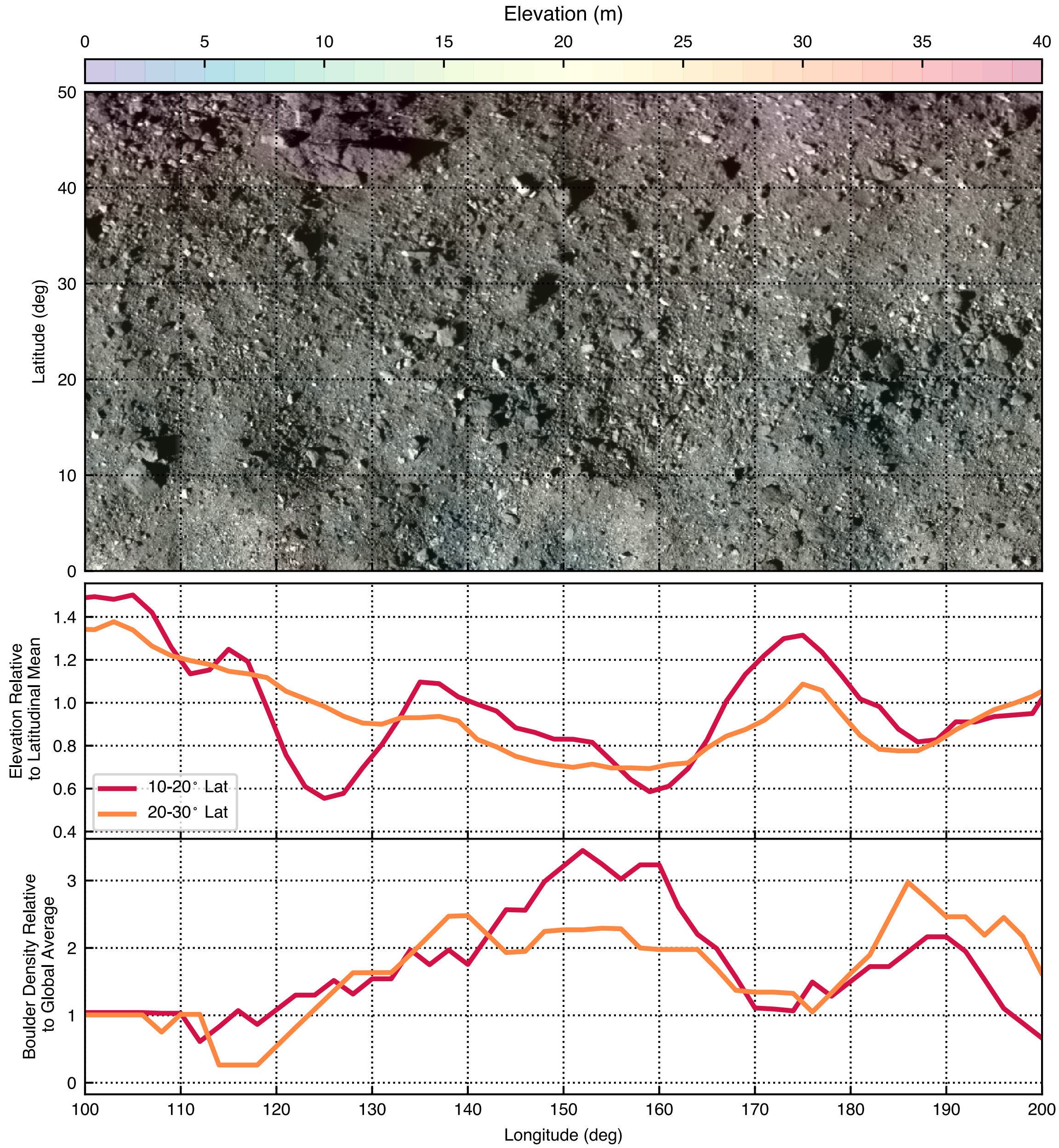

Supplementary Figure 4: Longitudinal ridges influence the density of large boulders. The density of boulders larger than 8 m is broadly controlled by the presence of the north-south longitudinal ridges that influence the global shape of Bennu (Fig. 1, 2, 3). Between the large ridges (near 100° and 180°, see also Fig. 3) the density of boulders is broadly enhanced along 10° bands of latitude. This strongly suggests mass wasting from the ridges is contributing to the boulder density between them.

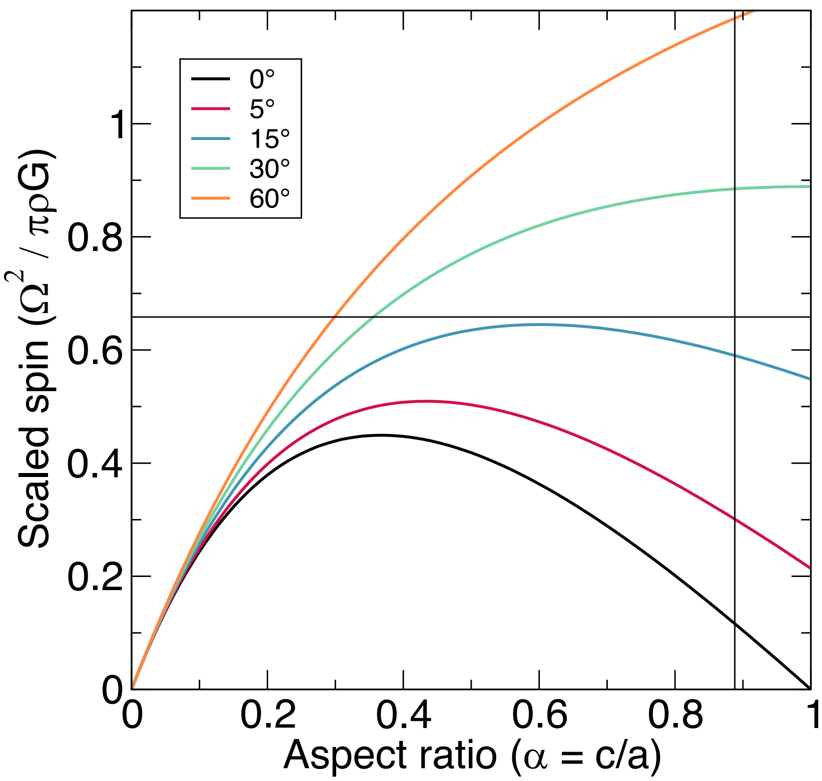

Supplementary Figure 5: Rotational stability for cohesionless, solid, oblate spheroids for a wide range of rotation rates, oblateness, and internal friction angles: Each curve describes the maximum dimensionless rotation rate as a function of aspect ratio (α = 1 is a sphere). Any solution below a curve is stable. The horizontal line marks the scaled spin value consistent with the with the observed density (~1.2 g cm^{-3}) and rotation rate of Bennu (4.3 h) [10]; under these conditions there are no stable solutions for a fluid body (lowermost curve). Some level of internal friction (or cohesion) is necessary to prevent Bennu from further flattening, and undergoing either despinning or binary fission. For a spheroid with Bennu's scaled spin parameter, a minimum friction angle of 18° satisfies the stability constraint.

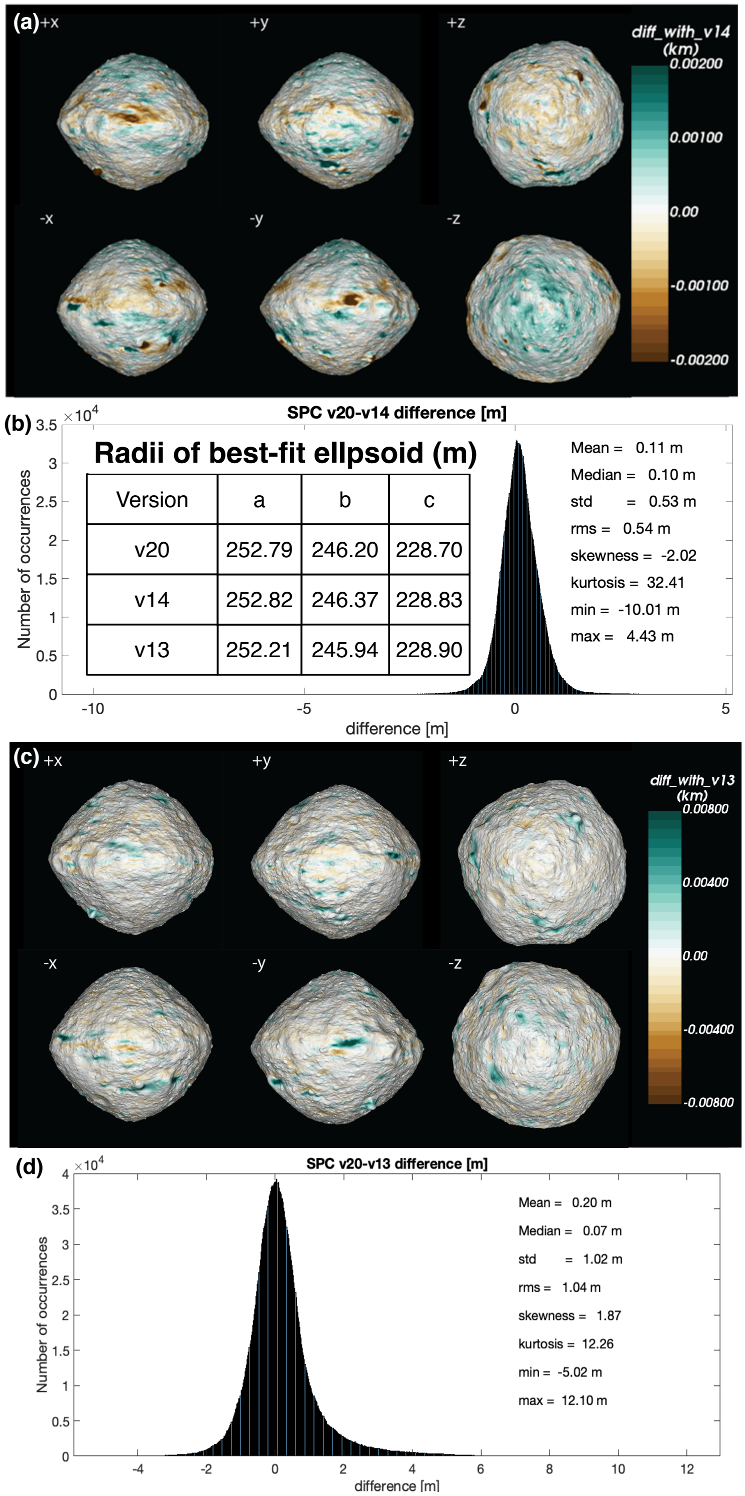

Supplementary Figure 6: Comparison of the current shape model (v20) of Bennu with two earlier version of the shape model (v13 and v14): The top panel shows how the models differ as a function of the location on Bennu, and the bottom panel provides a histogram of those differences and some statistics. The largest differences between the current and previous models are due to improvements in matching craters, boulders and other surface features where topography changes rapidly. As indicated by <0.25-m changes in the best-fit ellipsoid, Bennu's global shape was well determined in the earlier model. The v13 model has slightly better residuals when compared to OLA relative to v14, but v14 was developed using a well-tested set of procedures intended to safely navigate the spacecraft at Bennu. The v13 model was preferred for some of the investigations undertaken by the OSIRIS-REx science team because the improved modeling of surface blocks led to smaller residuals for image mosaicking and thermal studies.